HEMATITE AND CALCITE COATINGS ON FOSSIL VERTEBRATES

HUIMING BAO, PAUL L. KOCH,* AND ROBERT P. HEPPLE**
Department of Geosciences, Princeton University, Princeton, New Jersey 08544, U.S.A.
** Present address: Department of Earth Sciences, University of California, Santa Cruz, California 95064, U.S.A.*
*** Present address: Schlumberger Middle East S.A., P.O. Box 2836, Al-Khobar 31952, Kingdom of Saudi Arabia*

ABSTRACT: **Hematite coatings are common on vertebrate fossils from Paleocene/Eocene paleosol deposits in the Bighorn Basin, Wyoming. In general, hematite coatings are found only on fossils and are limited to soils exhibiting hydromorphic features and moderate maturity. Petrographic and isotopic evidence suggests that hematite and micritic calcite formed at nearly the same time in a pedogenic environment, whereas sparry calcite formed later at greater burial depths. The parent material of paleosols is rich in iron, supplying an ample source of iron for hematite formation. Decomposition of animal tissues around bones may enhance the weathering of iron-bearing minerals in soils surrounding carcasses, while the bones might provide favorable sites for iron accumulation. The predominance of discrete smectite, together with regional geothermal history, suggests that burial temperatures have not exceeded 70°C. Hematite coatings on fossils can serve as a substrate for geochemical analysis in continental paleoclimatic research, owing to their pedogenic origin, abundance, and resistance to diagenetic alteration.**

INTRODUCTION

Calcite, iron oxides, and manganese oxides often occur as coatings on the surfaces of fossil vertebrates. Encrustation is often so pervasive that details of bone and tooth morphology are obscured. Many vertebrate fossils from Cretaceous, Paleocene, Eocene, and Oligocene sediments in North America have iron oxide coatings (H. Bao, personal observation). Some examples are early and middle Paleocene fossils from New Mexico, Colorado, and Utah; Eocene fossils from the San Jose Formation, New Mexico; and early Oligocene fossils from the Brule Formation, South Dakota. The heaviest iron oxide coatings are on fossils from the late Paleocene and early Eocene paleosols of the Willwood Formation, Bighorn Basin, Wyoming, which are the focus of this study (Fig. 1). Here, we examine the genesis of Bighorn Basin hematite (α-Fe_2O_3) coatings in order to assess their suitability as substrates for geochemical analysis and for reconstruction of continental paleoclimate.

Our investigation of the formation of hematite coatings has two goals. First, hematite in paleosols may provide information on Paleocene/Eocene soil development and climate in the western interior of North America. The formation of different phases of iron oxides in soils is related to soil and climatic conditions (Schwertmann 1971, 1985; Schwertmann et al. 1982; Fitzpatrick and Schwertmann 1982; Fitzpatrick 1988). It is generally accepted that goethite forms under cool/wet conditions in organic-rich soils, while hematite forms under warm/dry conditions in organic-poor soils, although the actual conditions of formation may be more complicated (Schwertmann 1966, 1971, 1985; Wang and Hsu 1980; Schwertmann and Murad 1983; Schwertmann and Taylor 1989). However, hematite coatings on fossils differ from more common forms of soil iron oxides, such as iron oxide nodules and scattered fine crystals in bulk soil matrix, and their genesis has not been investigated extensively.

Second, oxygen isotope analysis of authigenic soil minerals has been a powerful tool for reconstruction of continental climates. Most studies, however, have been restricted to clay minerals and carbonates, particularly soil calcite and carbonate in biological minerals (Lawrence and Taylor 1972; Yapp 1979; Goodfriend et al. 1989; Lawrence and Rashkes Meaux 1993; Quade et al. 1989; Cerling and Quade 1993; Dettman and Lohmann 1993; Koch et al. 1995; Stern et al. 1995; Liu et al. 1996). Iron oxides have shown great potential as an alternate source for isotopic study (Yapp 1987, 1993a, 1993b). Before using oxygen isotope composition of iron oxides as a paleoclimatic indicator, it is crucial to understand how and when these oxides formed, and what burial conditions they experienced following formation. On the other hand, oxygen isotope data of hematite can be evidence for formation conditions. However, because of very different analytical procedures and discrepancies in the literature regarding the hematite–water fractionation relationship, reporting hematite isotope values is beyond the scope of this paper.

PALEOCLIMATIC AND GEOLOGICAL BACKGROUND

The Paleocene/Eocene transition has long been a focus in paleoclimatic research. Marine and land proxies suggest that the late Paleocene to early Eocene was one of the warmest time intervals in the Cenozoic (Shackleton and Kennett 1975; Savin 1977; Wolfe 1978, 1994; Miller et al. 1987; Stott et al. 1990; Wing et al. 1991; Zachos et al. 1993; Markwick 1994). In continental interior of western North America, paleontological evidence, such as the presence of palms, crocodiles, and turtles (Wing 1991 and references therein) suggests a warm climate. Mean annual temperatures ranging from 10 to 18°C have been suggested for the Paleocene/Eocene in Wyoming, on the basis of leaf physiognomy (Wing et al. 1991; Wing et al. 1993). Strong annual variations in $\delta^{18}O$ values of freshwater bivalves imply that a seasonal change in meteoric water supply occurred in this region (Dettman and Lohmann 1993).

The Bighorn Basin, northwest Wyoming, is a structural and topographic basin surrounded by several mountain ranges uplifted (Beartooth, Bighorn, and Owl Creek ranges) or erupted (Absaroka Range) from late Cretaceous to middle Eocene time in the Laramide orogeny (Fig. 2). Regional epeirogenic uplift of the area began in the late Oligocene or early Miocene, resulting in the erosion or nondeposition of sediments of Oligocene, Miocene, and younger ages (Bown 1980). Paleocene and Eocene fluvial and lacustrine deposits (up to 2000 m thick) are extensively exposed throughout the basin. In the southern and central Bighorn Basin, the stratigraphic position is measured relative to the base of the Willwood Formation, while in the northern Bighorn Basin, the stratigraphic position is relative to the base of the Paleocene Fort Union Formation (Fig. 2).

Paleosols are well developed on overbank and flood-plain deposits, and their distribution and development have been studied in detail (Van Houten 1944; Bown 1979; Bown and Kraus 1981a, 1987, 1993; Kraus 1987; Kraus and Bown 1988, 1993; Kraus and Aslan 1993; Bown et al. 1994). The A horizons of the paleosols are rarely preserved but are characterized by their deep gray color. B horizons can be divided into an upper B horizon, which is gray-purple, or pale purple to red, and a lower B horizon, which is lighter red, orange, or yellow. Paleosols have been assigned to different relative maturity levels (0–6) on the basis of properties observed in the field, including horizonation, profile development and thickness, color, soil-nodule development, mottling, and the nature of contacts within the profile (Bown and Kraus 1987). Combined A and upper B horizon thickness is regarded as one of the most characteristic factors in recognizing maturation stages.

Hydromorphic soils are common in the Willwood Formation. Soil hydromorphy is characterized by mottles (red, yellow-brown, and gray in color), slickensides, and in some cases, the presence of millimeter-size iron oxide nodules (Kraus and Aslan 1993). These hydromorphic features sug-

JOURNAL OF SEDIMENTARY RESEARCH, VOL. 68, NO. 5, SEPTEMBER, 1998, P. 727–738
Copyright © 1998, SEPM (Society for Sedimentary Geology) 1073-130X/98/068-727/$03.00

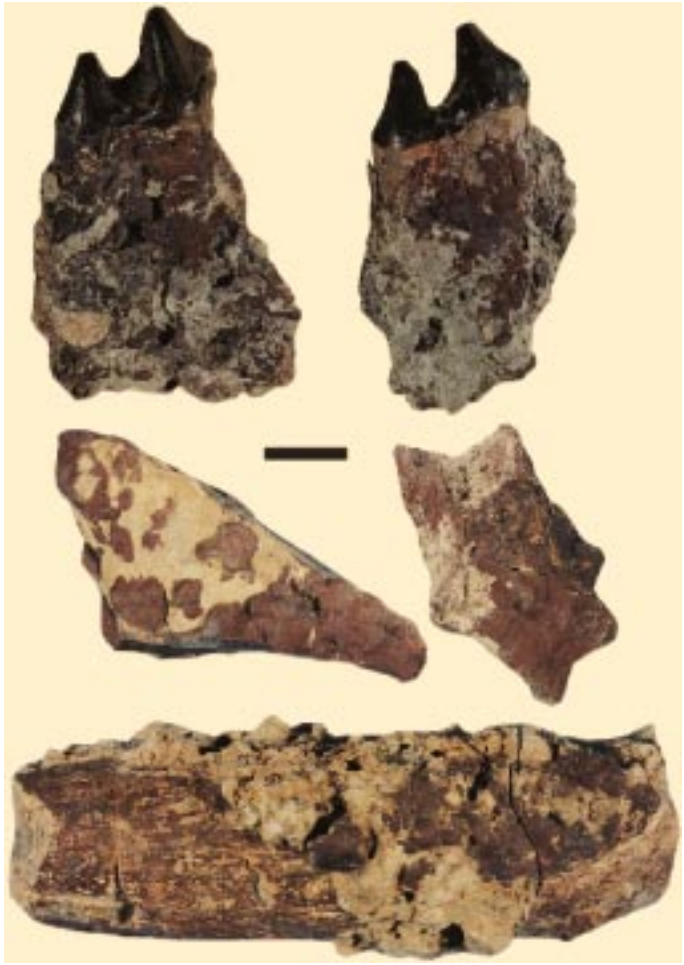

FIG. 1.—Hematite (purple-red) intimately mixing with pedogenic micrite (light-gray), or hematite as the dominant mineral occurring as coatings on vertebrate fossils from the Bighorn Basin, Wyoming. Scale = 1 cm.

gest that soils experienced alternating wet and dry cycles and associated alternations in reducing and oxidizing conditions, which resulted in the mobilization of elements such as Fe, Mn, Ca, and P (Bouma et al. 1990; Vepraskas and Guertal 1992). Lateral and vertical relationships of Bighorn Basin paleosols suggest that soil development was often terminated by episodic, rapid crevasse-splay deposition (Kraus 1987; Kraus and Bown 1988) and that each soil may represent thousands to tens of thousands of years, depending on its maturity.

Bown (1979) recognized 10 varieties of nodules and concretions from the Lower Willwood Formation. Soil carbonate nodules are present throughout the soil profile but are most common near the bottom of the B horizon. Red-purple hematite coatings with a brilliant-red streak are found exclusively on fossils. High concentrations of hematite are not observed in the soil matrix or on other kinds of soil nodules, including calcitic or apatitic nodules. Calcite is also present as overgrowths on fossils, and hematite and calcite coatings are intimately mixed. As reported by Bown (1979), concretions with deep purple iron oxide are ''almost entirely restricted to gray mudstone and nearly always associated with fossil vertebrate remains''. Bown and Kraus (1981a, 1981b) reported that most large concentrations of vertebrate fossils in the Willwood Formation in the southern and central Bighorn Basin are in widespread, tabular, thin (2 cm to 1 m) greenish- and bluish-gray mudstones that are consistently above mottled purple-and-orange mudstones. The gray mudstone was described as Class A gray mudstone and was thought to be relicts of the A horizons of ancient soils (Bown 1979; Bown and Kraus 1981a, 1981b). The restriction of hematite-coated fossils to gray mudstone strongly suggests that hematite formed in close association with soil processes.

Hematite-coated vertebrate fossils are common in the 120–580 m level in the southern and central Bighorn Basin, and in the 1100–1850 m level in the northern Bighorn Basin, but are encountered only sporadically outside of these intervals (Fig. 2). There is an $\sim$ 0.7 m.y. overlap in the very early Eocene among hematite samples from different parts of the basin. This restricted occurrence of hematite coatings may be related to temporal differences in soil maturity and hydromorphy (Bown et al. 1994). For example, in the southern Bighorn Basin, highly mature soils in the lower Willwood Formation (0–100 m), indicating low rates of sedimentation, are followed by moderately mature soils in the next several hundred meters (Bown and Kraus 1993). Hematite coatings are abundant in the moderately mature soils, but are relatively rare below the 100 m level, where soils developed over a considerable length of time. Overall, the association of hematite coatings with variations in paleosol conditions can be viewed as evidence of their pedogenic origin.

Goethite (α-FeOOH) nodules (with diameters of 0.1–5 mm) are found in some soil horizons, especially in the Elk Creek area of the Bighorn Basin (Kraus and Aslan 1993). We also found lepidocrocite (γ-FeOOH) in the center of one type of carbonate–hydroxylapatite nodule. The overall distribution of these iron oxide nodules in the basin is not well known. The presence of different phases of soil iron oxides indicates that different micro-environments may be responsible for their formation.

METHODS

Twenty-one polished thin sections were prepared from 16 calcite/hematite-coated fossil fragments from different stratigraphic levels in the southern and northern Bighorn Basin (Table 1). Thin sections of four soil carbonate nodules ranging from $\sim$ 250 to 500 m in the southern Bighorn Basin were also prepared. Petrographic examination included both transmitted and reflected light. Cathodoluminescence (CL) (model CCL 8200 mk3) was used for further determination of mineral overgrowth relationships at approximately 18 kV and 400 μA gun current. Freshly broken mineral surfaces were examined by scanning electron microscopy (SEM) (model ISIWB6 at 10 kV) to observe the crystal features of hematite.

Calcite and hematite coatings were drilled from the surfaces of fossils under a binocular light microscope. Clay minerals were obtained from bulk soils by gravity sedimentation (Jackson 1969) and also from hematite coatings by selective dissolution of hematite with 5 *M* HCl at 80°C for 30 min. A magnetic fraction was obtained from one bulk sample of a purple-red paleosol B horizon (SC303, 2110 m, northern Bighorn Basin) by high-gradient magnetic separation (HGMS) (Schulze and Dixon 1979).

Clay-mineral compositions from 27 soil horizons and 9 carbonate nodules, covering most of the Paleocene/Eocene stratigraphic levels in the basin, have been determined by standard methods from air-dried, ethylene-glycol-solvated, and heated (450°C for 12 hr) preparations (Hepple 1995). Clay minerals in hematite coatings were also analyzed for drilled powder and HCl-treated residues. X-ray diffraction (XRD) patterns were obtained using a Scintag PAD-V θ-2θ diffractometer with a Cu Kα radiation source at a scan rate of 1° or 2° 2θ/min. Identification of smectite/illite mixed-layer was conducted on 33 clay samples using Moore and Reynolds' (1989) method based on $\Delta 2\theta$ between the reflection of 001/002 (near 9° 2θ) and 002/003 (near 16° 2θ) of the ethylene-glycol-solvated samples, with $\pm$ 5% error.

The total iron contents and their variations in some paleosol profiles from the basin have been determined by Kraus and Aslan (1993) by acid digestion. In a study of the oxygen isotope composition of hematite coatings, we measured the Fe_2O_3 content of 20 coatings from different stratigraphic levels in the Bighorn Basin following treatment with 5M NaOH at 95°C to 100°C for 3 hr. Elemental concentration was measured using inductively

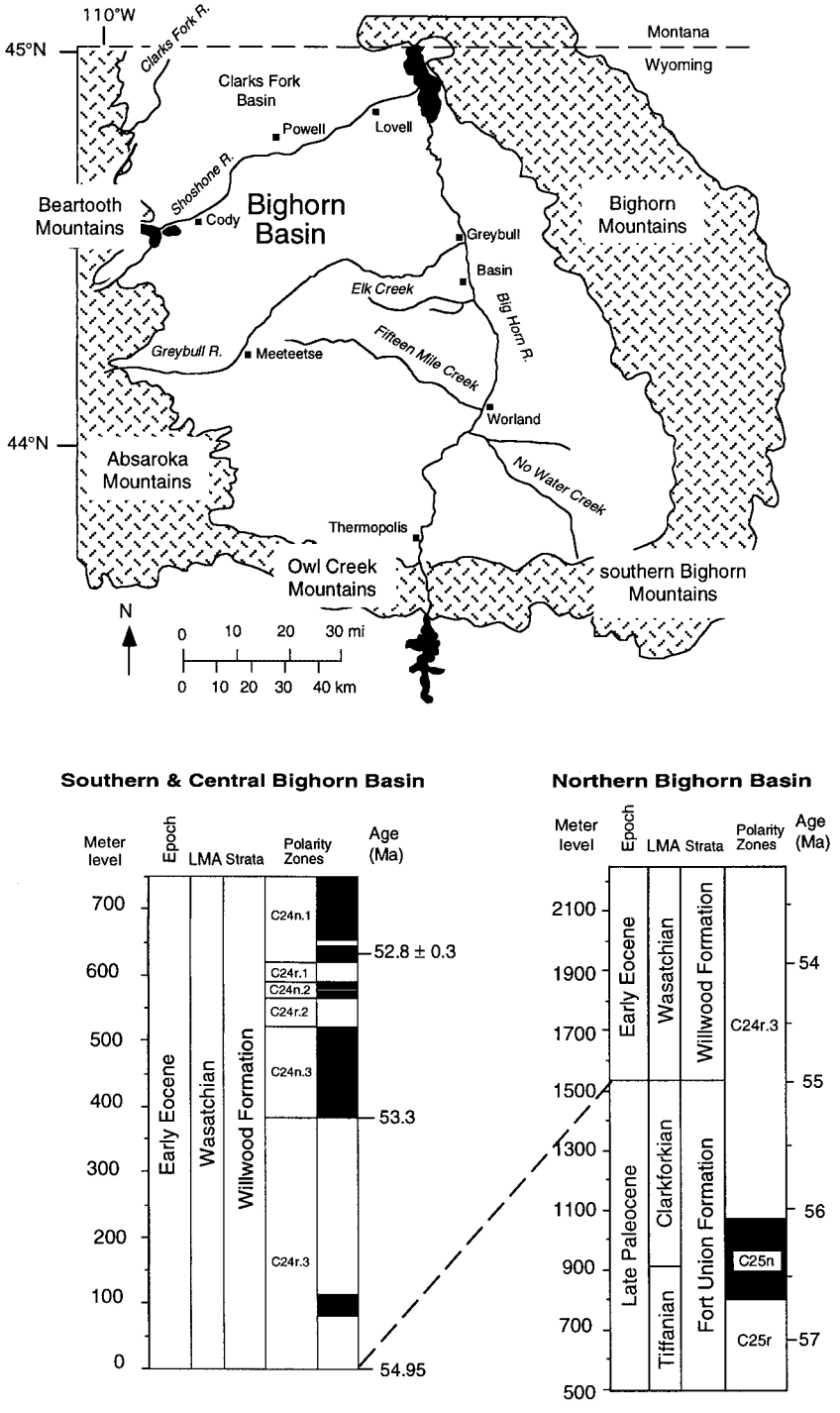

FIG. 2.—Map of the Bighorn Basin (from Koch et al. 1995), Paleocene/Eocene stratigraphic levels, North American Land Mammal Age (LMA), and estimated absolute ages (based on Wing et al. 1991, Clyde et al. 1994, Tauxe et al. 1994, and Koch et al. 1995) in both parts of the basin.

coupled plasma–atomic emission spectroscopy (ICP-AES) (Perkin Elmer 6000). The analytical error for duplicates in the wet chemistry procedures is ± 1%.

Oxygen and carbon isotope compositions were determined for bulk calcite coatings and microsamples of different generations of calcite on fossils. Bulk calcite coatings were drilled under a binocular microscope, and 2–4 mg samples were used. We analyzed 22 calcite coatings ranging from ~ 140 to 550 m in the southern basin and from ~ 1090 to 1850 m in the northern basin (Fig. 2). Microsampling of different generations of calcite was undertaken from polished thin sections following identification of different generations via light microscopy and cathodoluminescence. Samples (10–50 μg) were obtained by a computer-controlled microdrill under a binocular microscope. Drilled areas were examined by transmitted-light microscopy to ensure that the samples were collected from a single generation of calcite. Microsamples were obtained from 55 spots on 16 thin sections from 9 fossil coatings and bones (Table 1), and 10 spots on 3 thin sections of soil carbonate nodules.

Sample powders were reacted with 100% H_3PO_4 at 90°C. The CO_2 generated by the reaction was purified cryogenically, then transferred to an isotope-ratio-monitoring mass spectrometer for analysis. Bulk micrite sam-

TABLE 1.—*Oxygen and carbon isotopic data of micrite (M), recrystallized micrite (RM), drusy spar (D), bone spar (S1), and fracture spar (S2) from fossil coatings and soil carbonates.*

Thin section	Meter level (m)*	Calcite generation	$\delta^{13}C$ (V-PDB)	$\delta^{18}O$ (V-SMOW)	Note
D1410-B	410–418	S1	−29.4	18.1	fossil bone
D1410-B	410–418	S1	−31.2	17.9	fossil bone
D1410-B	410–418	S1	−25.1	18.7	fossil bone
D1410-B	410–418	S1	−31.1	17.7	fossil bone
D1410-B	410–418	M	−11.7	22.5	fossil bone
D1410-B	410–418	M	−11.6	22.5	fossil bone
D1410-A	410–418	S1	−20.7	17.5	fossil bone
D1410-A	410–418	S1	−26.0	17.7	fossil bone
D1410-A	410–418	S1	−30.8	17.8	fossil bone
D1410-A	410–418	S1	−20.7	15.9	fossil bone
D1410-A	410–418	M	−11.2	22.5	fossil bone
D1931-A	315	M	−8.9	22.6	fossil coating
D1931-A	315	RM	−8.9	22.8	fossil coating
D1931-A	315	RM	−8.9	22.7	fossil coating
D1931-B	315	M	−8.9	22.5	fossil coating
D1931-B	315	S2	−12.7	13.8	fossil coating
D1931-B	315	RM	−9.1	21.9	fossil coating
D1374-B	336	S2	−12.5	12.7	fossil coating
D1374-B	336	RM	−9.0	22.0	fossil coating
D1374-B	336	RM	−8.9	22.1	fossil coating
D1374-B	336	S2	−11.3	15.5	fossil coating
D1374-B	336	S2	−12.3	13.2	fossil coating
D1374-A	336	S2	−12.5	13.0	fossil coating
D1374-A	336	RM	−8.3	23.1	fossil coating
80H7-8-3-A	?	S2	−12.5	11.8	fossil coating
80H7-8-3-A	?	M	−10.0	22.1	fossil coating
80H7-8-3-A	?	S2	−12.5	11.8	fossil coating
80H7-8-3-A	?	M	−10.4	21.4	fossil coating
80H7-8-3-A	?	S2	−12.4	11.8	fossil coating
80H7-8-3-A	?	M	−10.3	22.2	fossil coating
80H7-8-3-B	?	S2	−12.7	11.7	fossil coating
80H7-8-3-B	?	M	−10.3	22.0	fossil coating
80H7-8-3-B	?	M	−10.4	21.9	fossil coating
80H7-8-3-B	?	M	−10.0	22.1	fossil coating
80H7-8-3-B	?	S2	−12.5	12.2	fossil coating
D1716-E	397	S2	−12.5	13.0	fossil coating
D1716-E	397	M	−10.9	20.3	fossil coating
D1716-D	397	S2	−12.4	13.2	fossil coating
D1716-D	397	M	−10.2	21.8	fossil coating
D1716-B	397	M	−9.3	19.4	fossil coating
D1716-B	397	S2	−14.2	11.4	fossil coating
D1716-F	397	S2	−11.7	11.6	fossil coating
D1716-F	397	M	−9.5	21.8	fossil coating
D1716-F	397	M	−9.8	22.2	fossil coating
D1716-F	397	S2	−11.7	12.4	fossil coating
D1-1	0	S1	−9.3	13.8	fossil bone
D1-1	0	S1	−9.3	13.9	fossil bone
D1-2	0	S1	−6.3	18.9	fossil bone
D1-2	0	S1	−6.2	19.0	fossil bone
D1-2	0	S1	−6.2	18.9	fossil bone
SC40	1535 (north)	S2	−10.2	17.8	fossil coating
SC40	1535 (north)	M	−8.9	22.4	fossil coating
SC40	1535 (north)	M	−9.1	22.5	fossil coating
SC62	1380 (north)	RM	−8.8	22.4	fossil bone
D1493	344	M	−11.4	22.3	calcite nodule
D1493	344	D	−10.0	23.3	
D1493	344	D	−10.8	20.4	
D1493	344	S2	−11.3	17.4	
D1389	264	S2	−9.9	16.6	calcite nodule
D1389	264	M	−9.5	22.5	
D1434	496	S2	−11.2	11.8	calcite nodule
D1434	496	M	−10.5	22.4	
D1434	496	S2	−10.8	13.1	
D1434	496	M	−10.7	22.7	

* Meter levels refer to the southern and central Bighorn Basin unless otherwise noted.

ples were analyzed using a VG-Optima, and microsamples were analyzed using a VG-Prism equipped with an ISOCARB automated carbonate device. Measurements are reported as per mil related to V-PDB for carbon and V-SMOW for oxygen with precision of 0.1‰.

XRD, ICP-AES, and isotope analyses of bulk calcite coatings were conducted in the Department of Geosciences at Princeton University. CL, SEM, microsampling, and isotope analysis of different calcite generations from thin sections were conducted at the Department of Earth Sciences, University of California, Santa Cruz.

RESULTS

Iron Content and Mineral Composition

The weight percent of Fe_2O_3 in hematite coatings ranges from 51.7 to 90.4% ($\bar{x}$ = 77.9%, 1σ = 8.7%, n = 20). It should be noted that these values are higher than the original compositions because a fraction of the original silicate minerals was dissolved in hot NaOH treatment.

XRD patterns indicate that quartz, smectite, chlorite, and micas are the major minerals in the clay fraction of bulk soils, along with a broad amorphous phase at 10–15° 2θ. XRD patterns from calcite and hematite coatings reveal the same suite of minerals as in bulk soil, but with much higher concentrations of calcite or hematite. Hematite peaks are sharp and no goethite phase is present. The a dimension of the hematite unit cell, obtained from d(110), suggests no detectable Al substitution in the hematite lattice (Schwertmann et al. 1979; Singh and Gilkes 1992). The magnetic fraction obtained from HGMS contains mostly greenish chlorite (probably clinochlore-1MIIB), which seems to be more concentrated in the > 2 μm fraction than in the clay fraction. No hematite or goethite peaks are found in the XRD pattern of the magnetic fraction of the bulk soil.

XRD analysis of 36 paleosol and carbonate nodule samples from across the basin demonstrates that smectite is the dominant clay mineral, with minor amounts of illite and kaolinite. Among the three clay minerals, smectite concentration averages 91.3% (1σ = 5.6%), while illite and kaolinite average 2.4% (1σ = 1.3%) and 6.3% (1σ = 4.9%), respectively. Further examination for a possible smectite/illite mixed-layered component on 33 of the clay samples shows that 13 samples are pure smectite. All other samples contain less than 20% illite component (8 samples $<$ 5%, 3 samples from 5 to 10%, 6 samples from 10 to 15%, and 3 samples from 15 to 20%). The estimation is based on the °2θ difference (°Δ2θ) between 001/002 and 002/003 reflections of the ethylene-glycol-solvated XRD patterns (Moore and Reynolds 1989). The detection errors for this method are generally from 5% to 10%.

Calcite and Hematite Overgrowth Relationships

Both hematite and calcite occur as coatings on bone and tooth surfaces, as well as in voids inside these materials. Petrographic and cathodoluminescence observations demonstrate that two major forms of calcite are associated with bones: micritic calcite and sparry calcite. Micrite is dark gray under transmitted light. It is recrystallized in some regions, but original fabrics of micrite are typically still visible. Recrystallized micrite is often as nonluminescent as pristine micrite. One of the distinct microfabrics in micrite is a fibrous to radial-fibrous structure (Fig. 3). The radial fibrous structure is common in calcite coatings and is morphologically similar to *Microcodium*, a biological structure reported from soil carbonates (Klappa 1978; Freytet and Plaziat 1982; Monger et al. 1991). The spherical structures bearing radial fabric are 0.1–0.8 mm in diameter and often exist as large aggregates where the fibrous fabric is sometimes obscured by overlap. The origin of *Microcodium* and other fibrous fabrics has been attributed to calcite microcrystal precipitation within fungal or bacterial mucilaginous sheaths, thereby retaining the biogenic growth form (Poncet 1976; Klappa 1983; Phillips et al. 1987). The *Microcodium*-like structures reported here, however, are closely associated with vertebrate remains, not plant roots as suggested by Klappa (1978).

Spar associated with hematite and calcite coatings is clean and transparent. It occurs in two forms: drusy (''dog-tooth'') spar and equant spar (Fig. 4). Thin layers of drusy spar are occasionally seen growing on the edge of micrite. Equant spar is the dominant calcite cement filling fractures and voids. Two types of equant spar are present in terms of their locations (Fig. 5). ''Fracture spar'' fills large cavities, including cracks in bones, hematite,

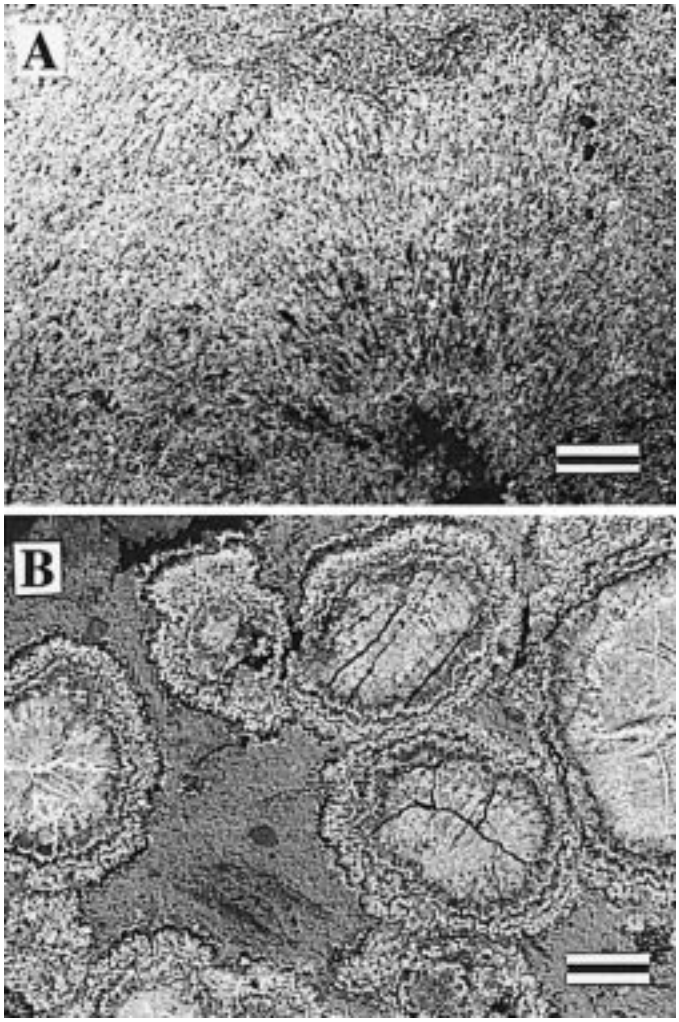

FIG. 3.—Photomicrographs of radial–fibrous fabrics in micrite from fossil coatings. **A)** Hematite in light color and micritic calcite in gray to dark gray color, reflected light. Scale = 0.05 mm (thin section D1374-B). **B)** Hematite as light-colored rings and micritic calcite as gray-colored rings on the edge of *Microcodium*-like spherical bodies, recrystallized micrite in light color in the center of the bodies; CL. Scale = 0.2 mm (thin section SC62).

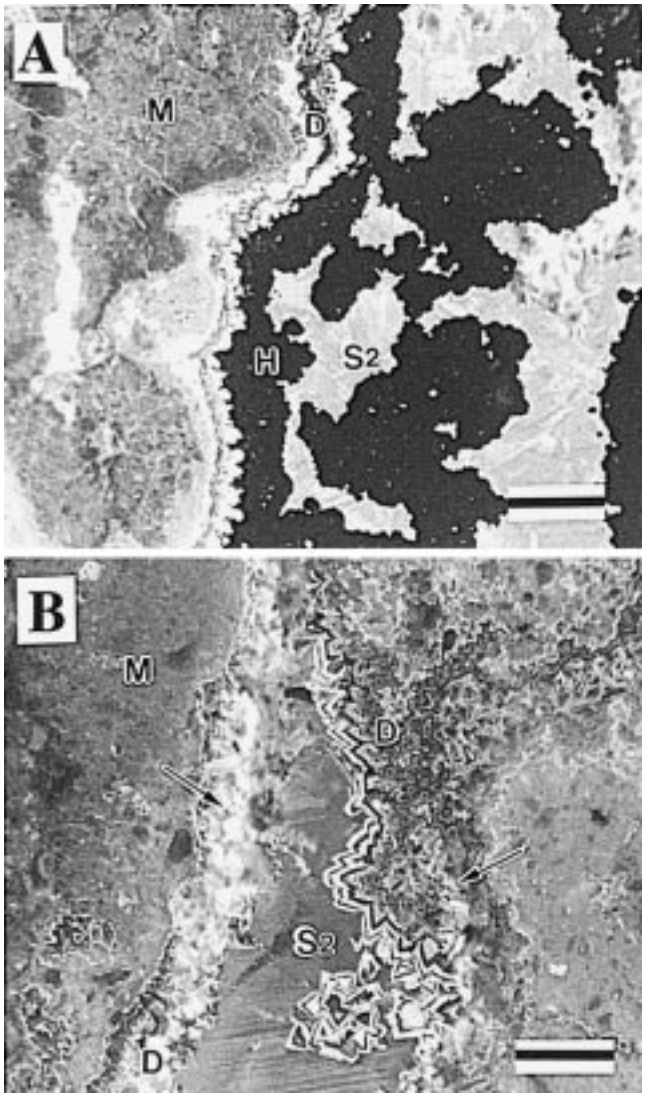

FIG. 4.—CL photomicrographs of micrite (M), drusy calcite (D), fracture-spar (S2), and hematite (H), with different luminescence patterns. **A)** Drusy calcite on the edge of micrite overgrown by hematite which is itself overgrown by sparry calcite; fossil coating (thin section D1931-A); **B)** drusy calcite on the edge of micrite overgrown by sparry calcite; notice the fuzzy strips (see arrows) in drusy calcite zones where microsamples have been taken for isotopic analysis; soil carbonate nodule (thin section D1495). Scale = 0.1 mm.

and carbonate coatings on bone (Figs. 4, 5A). ''Bone spar'' fills inter-trabecular spaces, osteons, and the marrow cavity inside bones (Fig. 5B). Some of the inter-trabecular spaces near the surface of bone can be filled up by hematite, but hematite coating is thinner or absent in the interiors of bone. Drusy spar shows a range of luminescence, from nonluminescent to dull to bright crystals (Fig. 4). Equant spar (including both fracture spar and bone spar) has a distinct brownish luminescence that is not as bright as that of typical drusy spar (Fig. 4). Calcite with similar morphologies and luminescence are found in Bighorn Basin soil carbonate nodules as well (Fig. 4B).

Hematite is found mixed with calcite and bone fragments both outside and inside bones (Fig. 1), and as thin coatings on micrite, bone, and drusy spar (Figs. 4A, 5). Different generations of hematite have not been observed. Fragments of bone apatite are common in the hematite matrix, especially in hematite that directly coats bone surfaces. Examination of thin sections of hematite under reflected light reveals a fibrous fabric similar to that displayed by fibrous micrite (Fig. 3). This observation indicates that partial replacement of fibrous micrite by hematite may have occurred. These hematites very likely precipitated after the formation of fibrous micrite (*Microcodium*-like structure).

Petrographic examination reveals that hematite and micrite are essentially cogenetic, and that both precede formation of equant spar. Micrite, particularly the fibrous micrite, is often seen overgrown by hematite (Fig. 5A). Alternatively, thin layers of hematite on bone are occasionally overgrown by micrite (Fig. 5B).

Detrital quartz and clay minerals are widespread in both hematite and micritic calcite, but are not seen in equant spar, suggesting that hematite and micrite formed in bulk soil matrix with some conservation of initial volume, while spar formed in void spaces resulting from fracturing or from removal of organic matter.

In summary, petrographic examination reveals that micrite, drusy calcite, and hematite are nearly contemporaneous, perhaps with hematite dominating the later stages, followed by filling of remaining voids and fractures by equant spar.

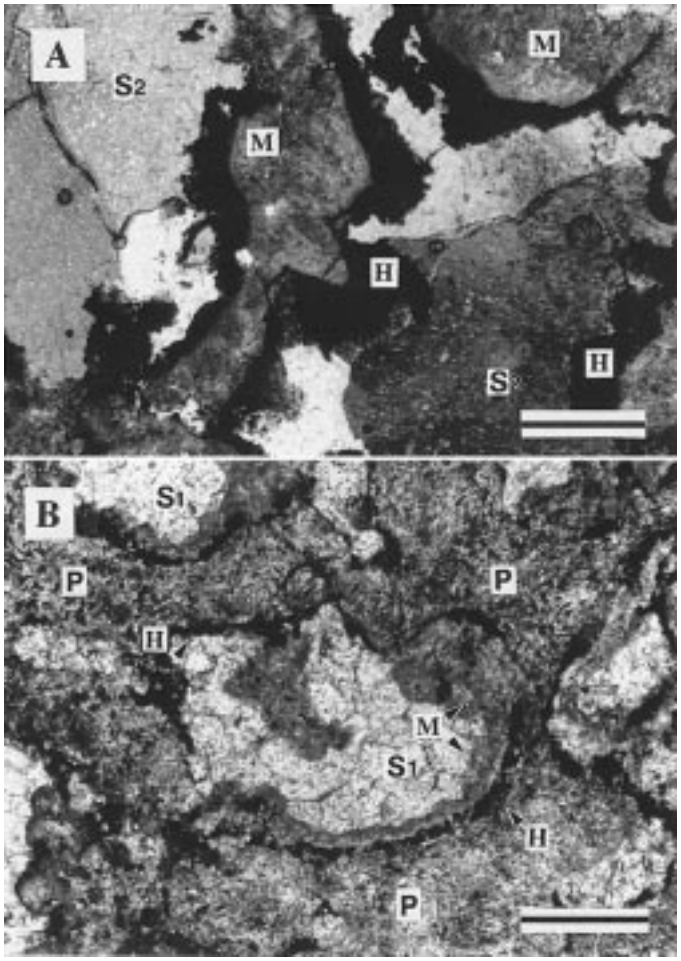

FIG. 5.—Photomicrographs showing the overgrowth relationship among hematite (H), micrite (M), bone spar (S1), fracture spar (S2), and bone (P). **A)** Micrite coated by hematite that is overgrown by spar (thin section of fossil 80H7-8-3-A), cross-polarized light; **B)** bone coated by hematite which is overgrown by micrite; bone spar filling inter-trabecular spaces (thin section of fossil D1410-B), plane-polarized light. Scale = 0.3 mm.

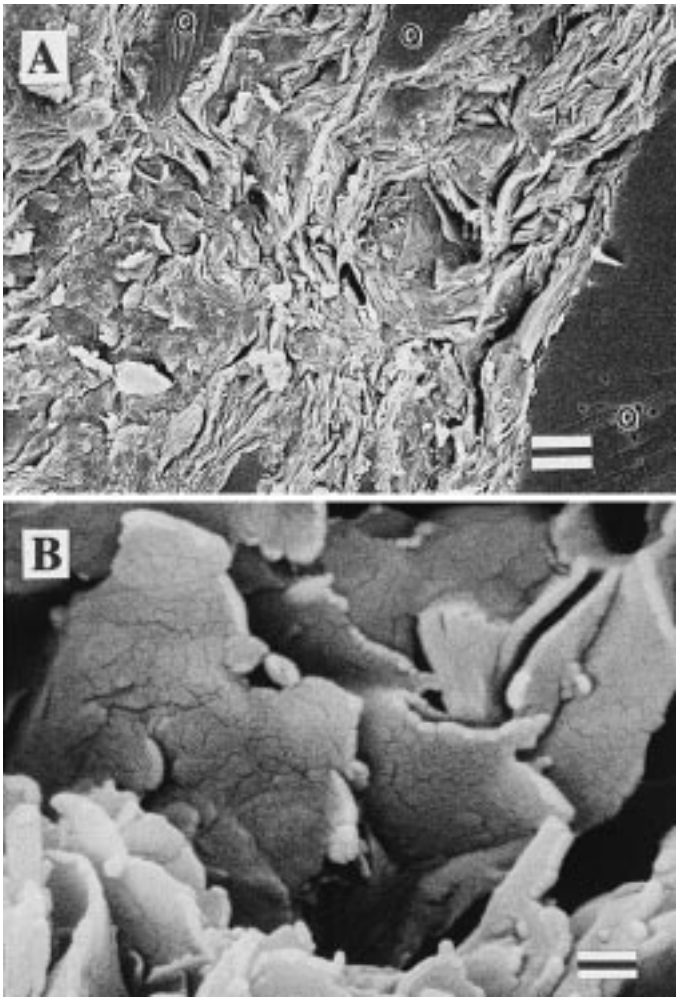

FIG. 6.—SEM micrographs of hematite coating. **A)** Platy and wavy hematite crystals (H) between detrital quartz grains (Q), scale = 2.8 μm; **B)** slightly bent hematite crystals with voids in between, scale = 0.28 μm.

SEM Observation of Hematite Coatings

Hematite crystals have a general platy morphology. Layers of hematite crystals are stacked and are parallel to each other locally (Fig. 6). Hematite plates are mostly irregular and do not have a well-developed hexagonal form. Most plates are somewhat curved or bent, resulting in enlarged and irregular spaces (0.02–0.2 μm) between some platy crystals. No hematite pseudomorphs after calcite, siderite, or clay minerals are observed.

Oxygen and Carbon Isotopes in Calcite

The ranges of $\delta^{13}C$ and $\delta^{18}O$ values for bulk micrite are -7 to -10.5‰ ($\bar{x} = -9.0$‰, $1\sigma = 1.1$‰, $n = 22$) and 20 to 23.1‰ ($\bar{x} = 21.9$‰, $1\sigma = 0.8$‰, $n = 22$), respectively. The ranges of carbon and oxygen isotope values of calcite coatings are the same as those for micritic calcite from soil carbonate nodules (Koch et al. 1995). We did not measure the isotopic composition from bulk samples of equant spar from hematite or micrite coatings on fossils. However, bulk data for sparry calcite from soil carbonate nodules reported by Koch et al. (1995) and Hepple (1995) are more scattered, with $\delta^{13}C$ values ranging from -2.5 to -18.4‰ and $\delta^{18}O$ values from 13 to 22.8‰.

Because petrographic examination demonstrated that different generations of calcite are intimately mixed, it was necessary to microsample each component to obtain pure isotopic compositions. Isotopic analysis reveals three distinct phases of calcite formation: micrite, bone spar, and fracture spar (Tables 1, 2; Fig. 7). Micrite microsamples from bones, including those with fibrous fabric, exhibit a narrow range of isotopic values similar to those for soil carbonates. Interestingly, the $\delta^{18}O$ value of recrystallized micrite is similar to that of pristine micrite, on the basis of six microsamples from three different fossil coatings. Likewise, two drusy calcite samples obtained from one soil carbonate nodule are similar in isotopic composition to the micrite they overlie. However, because of sampling resolution, we have not been able to sample pure drusy calcite from fossil-coating minerals. Equant bone spar and fracture spar have $\delta^{18}O$ values about 4.4‰ and 9.7‰ more negative than those of micrite, and $\delta^{13}C$ values $>$ 10‰

TABLE 2.—*Ranges, average values, and standard deviations of $\delta^{18}O$ and $\delta^{13}C$ of the three different calcite generations on fossil coatings.*

		Range		Average ± 1σ	
Calcite	n	$\delta^{18}O$	$\delta^{13}C$	$\delta^{18}O$	$\delta^{13}C$
micrite	18	19.4 to 22.6‰	−8.6 to −11.6‰	22.0 ± 0.8‰	−10.1 ± 0.9‰
bone spar	13	13.8 to 18.7‰	−6.2 to −31.2‰	17.4 ± 1.8‰	−19.4 ± 10.5‰
fracture spar	16	11.3 to 17.8‰	−10.2 to −12.7‰	12.9 ± 1.7‰	−12.5 ± 0.8‰

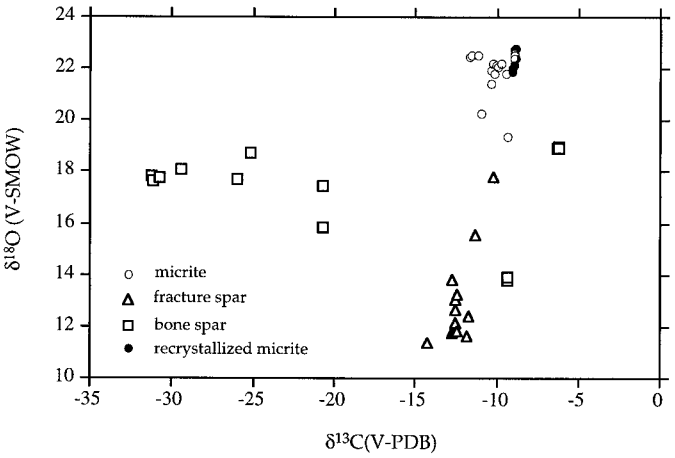

FIG. 7.—Plot of $\delta^{18}O$ versus $\delta^{13}C$ for different calcite generations in coatings on fossils from the Bighorn Basin, Wyoming.

and 2.3‰ more negative than those of micrite, respectively. Bone spar shows a large range of $\delta^{18}O$ and $\delta^{13}C$ values. At one end, their values are similar to fracture spar, while at the other end, they exhibit extremely low $\delta^{13}C$ and intermediate $\delta^{18}O$ values (Fig. 7).

DISCUSSION

Hematite is common in modern soils, especially in tropical regions. It occurs as a fine-grained mineral disseminated in the soil matrix, or as iron oxide crusts and nodules in certain horizons. There are no reported recent examples of iron oxide coatings on bone, except for red-brownish coatings of unknown composition on some archaeological bones (B. Nicholson, Brandon University, personal communication). The exclusive presence of highly concentrated hematite on fossils suggests a genetic relationship between hematite and fossils. Soil conditions and climates may be important factors in its genesis as well. We will discuss the following issues regarding the genesis of hematite coatings: (1) sources of iron, (2) mode of formation, (3) time of formation, (4) burial conditions, (5) possible geochemical scenarios for formation, and (6) pedogenic and paleoclimatic conditions that contribute to hematite formation. Finally, we consider the implications of these aspects of hematite genesis on the use of the oxygen isotope composition of hematite in paleoclimatic and paleohydrologic studies.

Sources of Iron

The iron in hematite coatings could be supplied by several different sources, such as hydrothermal fluids, upwelling of reduced groundwater, and dissolution and remobilization from iron-bearing minerals in the soil parent material. A hydrothermal source is unlikely, because it cannot explain the sporadic, fossil-associated, and paleosol-specific presence of hematite coatings in the Bighorn Basin. Seasonal fluctuations in soil moisture and associated change in redox conditions promote the release of iron ions from iron-bearing minerals and early pedogenic iron oxides. Iron in solution, from either deeper groundwater or local dissolution, may be transported or diffuse vertically and laterally, and may ultimately precipitate at oxidizing sites within the soil profile. Several lines of evidence support a local source for iron in hematite.

Kraus and Aslan (1993) reported that various kinds of Bighorn Basin paleosols have a high total iron content, with Fe_2O_3 ranging from 4 to 9 wt %. Magnetic separation of the clay fraction from the B horizon of a typical Bighorn Basin paleosol demonstrates that iron-bearing chlorite is a significant component. The proximity of these overbank fluvial deposits to upland sediment source regions probably explains their richness in easily weathered iron-bearing parent materials. Except for sandstone layers, iron content is quite uniform in soil profiles. The presence of mottles demonstrates that iron did migrate within paleosol horizons, but the overall uniformity of concentration within profiles indicates that little vertical remobilization of iron occurred within buried stacks of paleosols (Kraus and Aslan 1993). A groundwater source is less likely because coexisting pedogenic carbonates generally accumulate above the water table.

Given the average content of iron in bulk soil matrix (7 wt % Fe_2O_3), the formation of 1 g of hematite coating (70 wt % Fe_2O_3) on bone would require complete weathering of iron-bearing minerals in only 10 g of bulk soil. Therefore, even in a situation where extensive lateral and vertical transportation of iron is limited, the iron-rich soils adjacent to animal remains can provide sufficient iron for precipitation of highly concentrated hematite coatings. This hypothesis can be tested by examination of the hematite-coated fossils *in situ* (though this test is not possible here because our samples were obtained from museum collections). The iron content of the soil matrix immediately adjacent to the hematite coating should be lower than that at a distance, and the clay-mineral composition may be different as well, if post-pedogenetic processes have not homogenized the soil matrix.

Mode of Hematite Formation

The initial formation of soil iron oxides can proceed by at least two different pathways in terms of the crystal forms of precipitated iron oxides: (1) direct precipitation of iron-organic complexes or poorly crystalline iron oxides, which age to more crystalline iron oxide phases by decomposition, dehydration, or structural reorganization, and (2) dissolution and transformation of parent-rock silicates and kaolinite by iron oxides. The first pathway is the most common and occurs in soils under many different climatic regimes. These initial iron oxides mature to distinct final crystal forms and mineralogies (hematite, goethite, or lepidocrocite) depending on chemical conditions. The second pathway occurs mainly in tropical laterites. These iron oxides tend to have high substitution of Al for Fe (5–14 mole % Al) and they often occur as pseudomorphs of replaced silicates (Nahon 1986; Nahon et al. 1989; Merino et al. 1993).

XRD reveals no significant Al substitution in Bighorn Basin hematite, and no hematite pseudomorphs of silicate minerals are observed under SEM. Instead, the bent hematite plates and the enlarged spaces between plates suggest that a volume decrease may have occurred during the transformation of a hydrated precursor phase (e.g., ferrihydrite) to hematite. These observations support the conclusion that hematite coatings formed via precipitation of a precursor phase, probably followed by dehydration, and that they were not derived from transformation of parent-rock silicates by pseudomorphic replacement. The unusual physical and chemical conditions around bones are the source of the concentrations of iron oxides, rather than an extended period of intense weathering.

Time of Formation

Petrographic and cathodoluminescence observations demonstrate that micrite and drusy calcite form earlier than equant fracture spar, which is probably a later precipitate formed at greater burial depths. The similarity in stable-isotope composition between calcite coatings on fossils and soil carbonate nodules indicate that, like micrite in carbonate nodules, micrite in calcite coatings formed in a pedogenic environment. Mineral overgrowth relationships further demonstrate that iron oxide and micrite are cogenetic, and that both predate equant spar.

Overgrowth patterns indicate relative time of formation, but they do not reveal whether iron oxide precipitation was limited to the surface environment or continued to greater burial depths. Isotopic data from microsamples of different generations of calcite provide further constraints on the timing, temperature, and possible depth of iron oxide precipitation. Using mean

$\delta^{18}O$ values of 22‰ for micrite, 18‰ for bone spar, and 12‰ for fracture spar, we can calculate the temperatures of the formation of equant spar using

$$1000 \ln\alpha = 2.78 \times 10^6/T^2 - 2.89$$

(Friedman and O'Neil 1977), where α is the oxygen isotope fractionation factor between calcite and water and T is temperature in K. We assume (1) that micrite formed at temperatures between 10° and 20°C, and (2) that the $\delta^{18}O$ of formation water did not change between the time of micrite formation and the time of spar formation. Using these assumptions the calculated $\delta^{18}O$ of formation water is between −7.5 to −10‰, and bone spar formed at a temperature between 28 and 40°C, whereas fracture spar formed at higher temperatures, between 60 and 80°C. The first assumption is based on independent paleoclimatic proxies, such as leaf physiognomy and faunal and floral composition recorded in the basin across the Paleocene/Eocene boundary (Wing et al. 1991; Wing et al. 1993). The second assumption is less well supported. If water at depth was enriched in ^{18}O in comparison to surface water, our temperature estimate for the spar formation would be too low, whereas if water at depth was ^{18}O-depleted, our estimated temperature would be higher than the actual temperature for spar formation.

No information is available on the $\delta^{18}O$ evolution of deep brines in the Bighorn Basin since the Paleocene. Present-day shallow groundwater $\delta^{18}O$ values are −15 to −17‰ at Riverton, Wyoming, and −16.3‰ at Douglas, Wyoming (Narasimhan et al. 1982; Lander 1991). However, the probable direction of any change in $\delta^{18}O$ of formation water with depth can be constrained by examination of modern soil carbonates. Deep vadose waters generally have $\delta^{18}O$ values close to the mean annual meteoric value for a region (Yonge et al. 1985). Recent studies have demonstrated that the $\delta^{18}O$ of soil water in equilibrium with modern soil carbonate is usually 2–10‰ heavier than that of local average meteoric water, depending on the climatic regime (Schlesinger 1985; Quade et al. 1989; Marion et al. 1991; Liu et al. 1996). The effect has been attributed to evaporative ^{16}O loss and/or a warm-season bias in soil carbonate formation. It is possible, therefore, that the $\delta^{18}O$ of water in equilibrium with ancient micrites is several per mil more positive than that of water at depth in equilibrium with spar. If we assume a 3‰ enrichment of soil water relative to deep water (the average enrichment for modern soils in upper midwestern North America; Cerling and Wang 1996), we calculate formation temperatures of 14–25°C for bone spar and 44–58°C for fracture spar, respectively. The temperature estimates for bone spar, which overgrows hematite, constrain iron oxide formation to the near-surface environment, which is cooler and shallower than the site of fracture-spar formation.

The very negative $\delta^{13}C$ values of bone spar suggest an origin related to sources of organic carbon. Several fractionation processes associated with organic-matter degradation can provide ^{13}C-depleted HCO_3^- for incorporation into bone spar. According to Irwin et al. (1977), bacterial aerobic oxidation, nitrate and iron reduction, and bacterial anaerobic sulfate reduction can all produce HCO_3^- with $\delta^{13}C$ value of $\sim$ −25‰ in a C_3 plant environment. Extremely ^{13}C-depleted HCO_3^- (as low as −75‰) can come from bacterial methane oxidation. On the other hand, bacterial methanogenic fermentation can provide rather ^{13}C-enriched HCO_3^- (+15‰) when ^{13}C-depleted methane is produced. Atmospheric CO_2 is also another relatively ^{13}C-enriched source ($\sim$ −7‰) for bone spar. Therefore, the large variation in the observed $\delta^{13}C$ of bone spar (from −6‰ to −32‰) suggests that different mixing ratios of the various HCO_3^- sources inside bone may have been responsible. Because the very negative $\delta^{13}C$ values have not been found in fracture spar, it is less likely that a later basinwide negative $\delta^{13}C$ source (such as CO_2 from thermally induced decarboxylation) is the cause of the observed bone spar $\delta^{13}C$ values. Our current data do not supply a full explanation of these carbon isotope variations or the exact source of ^{13}C-depleted carbon for bone spar. Nevertheless, the possible fractionation processes that provide ^{13}C-depleted HCO_3^- for bone spar must have operated relatively close to the surface during the early stages of diagenesis, when there was still significant organic-matter decomposition.

Therefore overgrowth and isotopic data for different generations of calcite demonstrate that hematite formed early, in the near-surface environment. This conclusion is consistent with the observation that iron oxide formation requires oxidizing conditions with O_2 as electron acceptor (Garrels and Christ 1965). While anoxic conditions normally hold only a few centimeters below the sea floor in marine sediments, oxidizing conditions can persist to much greater depths in continental sediments, particularly those that are organic-poor (Winograd and Robertson 1982). However, oxidizing groundwater is uncommon and is largely confined to actively recharged, sandy aquifers, because O_2 is often consumed in near-surface sediments by oxidation of organic matter and mafic minerals (Retallack 1991). It is difficult, therefore, to understand how oxidizing conditions, sufficient for the formation of highly concentrated hematite coatings, could exist at great depths in these clayey, organic-rich, hydromorphic soils in the Bighorn Basin.

Because this study was conducted on museum specimens, we were not able to sample hematite-encrusted fossils *in situ* from paleosols. We were concerned, therefore, that hematite coatings might have formed by recent weathering processes, when fossils were near the modern soil surface. Several lines of evidence preclude this possibility. The overgrowth of hematite by spar, which has a deep-burial origin, suggests that hematite was once deeply buried too. Study of vertebrate-fossil-bearing paleosols suggests that the time between exhumation and reburial or destruction of fossils is about 3–6 years in areas not covered by lag deposits or in excess of 10 years in areas where large lags occur (Bown and Kraus 1981b). It is difficult to form highly concentrated hematite coatings in such a short time in the highly erosional and arid badlands. Remnant mineral should be detected if the hematite coatings were transformed from an early mineral coating (e.g., siderite) by recent weathering. Large amounts of amorphous and poorly crystalline iron oxide would be expected in XRD analysis if hematite coatings were currently forming. However, no evidence of recent mineral transformation is found, and amorphous or poorly crystalline iron oxides are insignificant. We conclude, therefore, that recent formation of hematite is not convincing.

Burial Conditions

Sedimentary evidence suggests that regional epeirogenic uplift of the Bighorn Basin occurred in the late Oligocene or early Miocene, initiating erosional conditions and ultimately exposing the Paleocene/Eocene paleosols (Bown 1980). These paleosols may have been buried more than 1500 m below the surface in some parts of the basin. However, no definite information on burial depth or duration of deep burial is available.

We can calculate the maximum burial depths of the paleosols at the time of spar formation based on the geothermal gradient. According to apatite fission-track data, the maximum geothermal gradient permitted by thermal histories during post-Laramide time is 17°C/km, similar to the current geothermal gradient in this part of Wyoming, indicating that a low geothermal gradient has prevailed since the formation of Paleocene and Eocene soils (Omar et al. 1994). Using the estimated formation temperatures calculated above (which assume a 3‰ evaporative enrichment for micrite formation waters), the bone spar formed at depths of 235–295 m, and fracture spar formed at depths of 2000–2235 m. These inferred depths are quite sensitive to the assumed difference in $\delta^{18}O$ between surface water for micrite formation and deep water for spar formation. A higher ^{18}O enrichment for surface water would result in a shallower depth estimate for spar formation.

The clay-mineral composition of paleosols provides another line of evidence regarding burial conditions. The smectite-to-illite transition is kinetically controlled and is a function of time and temperature, as well as availability of potassium. The transition has been used as a geothermometer

to constrain the upper temperature limit of diagenetic or metamorphic processes (Hoffman and Hower 1979; Moore and Reynolds 1989; Pollastro 1990; Eberl 1993; Eberl et al. 1993). Paleosols in the Bighorn Basin have ample potassium (Kraus and Aslan 1993), and have been buried for 52 million years. Obviously, the illite/smectite clay-mineral data reveal minimal transition during this long interval. The lack of clay-mineral transformation suggests burial temperatures less than 70°C or a burial depth less than 2000 m, according to Hower (1981).

In hydrothermal systems, hematite can form through thermal dehydration of iron salts or a crystalline iron oxyhydroxide such as goethite (e.g., $2FeOOH \rightarrow Fe_2O_3 + H_2O$). High-temperature hematite usually has a large (1–3 μm) hexagonal plate crystal morphology (Schwertmann and Cornell 1991), which is not seen in hematite coatings. Furthermore hydrothermal hematite should occur in a pattern related to tectonic structures, rather than in a pattern controlled by conditions of paleosol formation.

Geochemistry

The association between hematite and fossils is intriguing. As explained by Bown and Kraus (1981a), ''they [hematite coatings] indicate local oxidizing conditions, and in Class A gray mudstones and related bone-bearing units, probably reflect oxidation and dehydration of amorphous ferrous iron compounds that were deposited on the bones''. No geochemical explanation, however, has been provided for the exclusive association of hematite and fossils. In this section, we try to provide possible geochemical scenarios for the preferential precipitation of hematite on fossils. We admit at the outset that further experimental study is needed to elucidate these processes.

During decomposition of animals a variety of organic acids are released, and a general acidic condition prevails that seems unfavorable for calcite precipitation. The presence of many calcite coatings on fossils may, however, be best explained by the models proposed by Weeks (1953) and Berner (1968, 1969). Rapid formation of bases adjacent to the decaying body may locally increase pH and induce precipitation of calcite. The bases, ammonia and volatile amines, are produced by deamination and decarboxylation of amino acids.

The early acidic condition and the large amount of organic acids present can greatly enhance the weathering rate of minerals in soil horizon, such as the Class A gray mudstones where animal remains were buried (Robert and Berthelin 1986). Iron-bearing minerals such as micas are among the minerals most susceptible to attack by organic acids (Tan 1986, 1989; Heyes and Moore 1992). Acid-enhanced weathering may have resulted in the release of large amounts of Fe(II) and Fe(III) from the iron-rich Bighorn Basin soil parent materials.

There are at least three probable mechanisms for preferential accumulation of iron ions around bones. First, the calcite that formed early on bones, and possibly bone apatite itself, may act as a favorable substrate for iron-oxide precipitation. Iron oxide is precipitated rapidly at elevated pH (Garrels and Christ 1965; Johnson and Swett 1974). A high pH may be present around bone in a generally acidic soil environment because of (1) the continued release of bases by decay processes and (2) the pH buffering role of calcite and apatite.

Second, released iron ions may not precipitate as iron oxides initially. Iron-organic complexes are probably the most common iron compounds in soils (Schwertmann et al. 1986; McKeague et al. 1986). The insoluble forms of iron–organic compounds tend to precipitate on mineral surfaces because of saturation of the organo-metal complexes (De Coninck 1980). It is, therefore, possible that iron may have accumulated first as iron–organic complexes around animal remains, and then was further oxidized to a stable oxide phase (Schwertmann and Fischer 1973; McKeague at al. 1986). Because O_2 is required for the subsequent oxidation of iron–organic complexes to iron oxides, this transformation should have occurred before animal remains were buried below the oxidizing zone in soils. The formation of insoluble iron–organic complexes around bones, as well as the formation of a solid iron-oxide phase in the first scenario, may have created a diffusion gradient that facilitated transport of additional iron ions to these sites of iron accumulation.

Third, as mentioned by Bown and Kraus (1981a), the initial precipitates around bones may have been ferrous iron compounds that were subsequently oxidized to ferric oxides. Siderite ($FeCO_3$) may precipitate on bones in HCO_3^--rich environments when conditions are slightly reducing (suboxic zone) or strongly reducing (methanogenic zone) (Mozley and Wersin 1992). This scenario is less likely because XRD and SEM examinations of hematite coatings reveal no traces of siderite or hematite pseudomorphs after siderite. If siderite did form in the early stages of soil development, it must have been completely dissolved and reprecipitated as iron oxide soon after oxidizing conditions prevailed in soils.

Goethite, a common iron-oxide phase in many soils, was not detected on our bone samples, but has been reported coexisting with hematite coatings on some Bighorn Basin bones (Bown and Kraus 1981a). The predominance of hematite on fossils in the Bighorn Basin is probably due to the abundance of calcite and HCO_3^-, which can inhibit the precipitation of goethite (Schwertmann and Cornell 1991).

Pedogenic and Paleoclimatic Controls on Hematite Formation

By analogy to modern soils, the accumulation of iron oxides in soils suggests generally wet soil conditions with at least moderate seasonal differences in soil moisture. However, iron-oxide coatings on vertebrate fossils are not ubiquitous in all depositional settings and times in earth history. The physical and chemical processes associated with decaying animals, a particular combination of sedimentation rates and soil processes, and Paleocene/Eocene climatic conditions in the Bighorn Basin must have acted in concert to provide an extremely favorable environment for hematite precipitation. The key features of soil and climate that may have contributed to the formation of hematite coating are (1) iron-rich soil parent materials, (2) hydromorphic soils (Bown and Kraus 1981a; Kraus and Aslan 1993), (3) warm temperature (Wing et al. 1991; Wolfe 1994; Greenwood and Wing 1995), (4) alternating wet/dry conditions and fluctuating water tables (Bown and Kraus 1981a; Kraus and Aslan 1993), (5) episodic flooding or rapid crevasse-splay deposition, which limited the time of soil development (Kraus 1987), and (6) favorable taphonomic conditions (i.e., bones mostly unweathered or rarely in advanced stages of decomposition when buried) (Bown and Kraus 1981b).

Implications For Paleoclimatic Reconstruction

The same two major generations of calcite (early micrite, later spar) are also observed in carbonate nodules from the Bighorn Basin. According to CL observations, recrystallized micrite is often as nonluminescent as micrite, indicating that recrystallization is an early transformation process that occurred in a setting similar to that of micrite formation. The recrystallized micrite probably retains an original soil-water signal, as suggested by our microsample data. Two of the drusy calcite samples from one soil carbonate nodule have isotopic values similar to micrite, but drusy calcite exhibits a range of luminescence. Equant spars exhibit a distinct brownish luminescence, and there is no obvious difference in luminescence between the two isotopically different spars (bone spar and fracture spar). CL observation is an effective tool for distinguishing different calcite generations but not for identifying materials with different carbon and oxygen isotope values. To make inferences about environmental conditions at the surface, only isotopic data from micrite and, perhaps, drusy calcite, should be used.

The $\delta^{13}C$ value of soil carbonate has widely been used as an indicator of changes in vegetation and atmospheric P_{CO_2} (Cerling 1992; Cerling and Quade 1993; Sinha and Stott 1994; Andrews et al. 1995; Ghosh et al. 1995; Mora et al. 1996). Yet the $\delta^{13}C$ of calcite is not identical between the different generations of calcite. For example, bone spar has very negative

$\delta^{13}C$ values. The fracture spar, which is more common in soil nodules, has $\delta^{13}C$ values $\sim$ 2‰ lower than micrite from the same carbonate nodule. Heterogeneity of soil carbonates due to diagenesis has also been reported (Monger et al. 1991; Deutz et al. 1995). Careful petrographic examination, together with microsampling from polished thin sections, should be undertaken in future carbon isotope studies employing soil carbonates.

Although the oxygen-isotope composition of paleosol carbonate has been used as a rough indicator of paleoclimatic change in a number of studies (Quade et al. 1989; Humphery and Ferring 1994; Ghosh et al. 1995; Koch et al. 1995; Liu et al. 1996), there are substantial uncertainties associated with the estimates of the $\delta^{18}O$ of meteoric water derived from this method. Three major problems are associated with application of the $\delta^{18}O$ of pedogenic calcite in paleoclimatic studies. (1) The $\delta^{18}O$ of calcite is determined by two variables: temperature, through its effect on α, and the $\delta^{18}O$ of water. (2) It is difficult to quantify or constrain the potential effects of evaporation or seasonal changes in soil water composition. (3) As demonstrated above, pedogenic calcite is frequently intermixed at a fine scale with diagenetic spar that has a very different $\delta^{18}O$ value. The potential for contamination by this diagenetic spar is great unless extreme care is taken in sample collection.

Hematite coatings provide a proxy for the $\delta^{18}O$ of soil water that is more robust in terms of all three problems affecting pedogenic calcite. Petrographic examination, clay-mineral analysis, and isotopic data reveal that hematite coatings on bone are pedogenic or shallow-burial products. There is no evidence for later formation of hematite in deep burial environments. Also, several studies have demonstrated that hematite is highly retentive of its original isotope composition. Becker and Clayton (1976) suggested that hematite underwent negligible isotope exchange with coexisting minerals in a Precambrian banded iron formation in Western Australia, while quartz and carbonates had almost completely equilibrated with one another at estimated temperatures of 270–310°C. Yapp's (1991) experiments uncovered no isotopic exchange between water and goethite over many hours in boiling 5 *M* NaOH solutions.

As mentioned above, evaporative and/or seasonal effects can have a significant impact on the $\delta^{18}O$ of soil carbonates (Quade et al. 1989; Marion et al. 1991; Liu et al. 1996). It is likely that typical soil carbonates form in equilibrium with soil pore fluids that are ^{18}O-enriched relative to meteoric water, though these effects have not been the subject of long-term systematic study (Cerling and Quade 1993). Even less is known about the water signal that is recorded by pedogenic iron oxides. For example, it is unknown whether soil oxides equilibrate with waters that reflect the long-term average, mean annual, summer, or rainy-season $\delta^{18}O$ values, and there are few studies of the $\delta^{18}O$ of modern soil iron oxides and local meteoric water (see Bird et al. 1992 and Yapp 1997 for exceptions). It is also possible that different types of pedogenic iron oxides have different relations to local meteoric water because of the difference in formation conditions and pathways. For example, goethite from lateritic regolith may be ^{18}O-enriched because of evaporation (Bird et al. 1992).

However, pedogenic iron oxides typically transform from poorly crystalline materials to highly crystalline minerals over a period of several thousand years (McFadden and Hendricks 1985; Fitzpatrick 1988; Schwertmann and Taylor 1989; Aniku and Singer 1990; Merritts et al. 1991). If the initial iron-oxide precipitates are quickly buried because of rapid sedimentation, long-term aging, which may involve dissolution and reprecipitation, may erase short-term seasonal and interannual variability in soil water, such that iron oxides retain a record of long-term average $\delta^{18}O$ values of shallow surface water.

Judging by the time and depth constraints on hematite formation deduced from petrographic and isotopic data, the water signal recorded by hematite coatings could be a long-term average of soil water and ground water at shallow burial depths (certainly less than 200 m) that represents an average signal of local meteoric precipitation. On the other hand, the presence of soil carbonate may have facilitated rapid crystallization of iron oxide during early stages of pedogenesis, such that hematite may have formed from solutions of evaporatively ^{18}O-enriched soil water. In the absence of independent evidence, it is imperative to understand the relationships among calcite, iron oxide, and water isotopic signals in modern soils.

CONCLUSIONS

We have proposed an interpretation for the formation of hematite coatings on vertebrate fossils, on the basis of Paleocene/Eocene samples from the Bighorn Basin, Wyoming. Evidence from field occurrence, petrographic examination, clay mineralogy, and stable-isotope analysis of coexisting calcite generations suggests that hematite coatings are a pedogenic to shallow-burial product and have experienced no more than 70°C burial temperatures during their 52 million year burial history. This early origin, coupled with their resistance to diagenetic alteration, make hematite coatings an ideal mineral for continental paleoclimate research. The primary inferred geochemical processes involved in the genesis of hematite coatings are decomposition of animal tissues, which enhances the release of iron from iron-rich minerals in adjacent soils, and the role of soil carbonate and bone mineral as buffers, which provide a stable microevironment for precipitation of hematite around bones.

ACKNOWLEDGMENTS

We thank T. Bown of USGS at Denver, and P.D. Gingerich and G. Gunnel at the Museum of Paleontology, University of Michigan, Ann Arbor, for providing us fossil samples. Technical assistance from Doug Yates, Doug Johnson, Jonathan Krupp, Bruce Tanner, and Geoff Koehler are gratefully acknowledged. This research is supported by National Science Foundation grant EAR-9627953 to PLK, and the Department of Geosciences, Princeton University. We thank M.J. Kraus, J. Quade, and C. Yapp for helpful reviews of this manuscript.

REFERENCES

Andrews, J.E., Tandon, S.K., and Dennis, P.F., 1995, Concentration of carbon dioxide in the Late Cretaceous atmosphere: Geological Society of London, Journal, v. 152, p. 1–3.

Aniku, J.R.F., and Singer, M.J., 1990, Pedogenic iron oxide trends in a marine terrace chronosequence: Soil Science Society of America, Journal, v. 54, p. 147–152.

Becker, R.H., and Clayton, R.N., 1976, Oxygen isotope study of a Precambrian banded iron-formation, Hamersley Range, Western Australia: Geochimica et Cosmochimica Acta, v. 40, p. 1153–1165.

Berner, R.A., 1968, Calcium carbonate concretions formed by the decomposition of organic matter: Science, v. 159, p. 195–197.

Berner, R.A., 1969, Chemical changes affecting dissolved calcium during the bacterial decomposition of fish and clams in sea water: Marine Geology, v. 7, p. 253–274.

Bird, M.I., Longstaffe, F.J., Fyfe, W.S., and Bildgen, P., 1992, Oxygen-isotope systematics in a multiphase weathering system in Haiti: Geochimica et Cosmochimica Acta, v. 56, p. 2831–2838.

Bouma, J., Fox, C.A., and Miedema, R., 1990, Micromorphology of hydromorphic soils: application for soil genesis and land evaluation, *in* Douglas, L.A., ed., Soil Micromorphology: Amsterdam, Elsevier, p. 257–278.

Bown, T.M., 1979, Geology and mammalian paleontology of the sand creek facies, Lower Willwood Formation (Lower Eocene), Washakie County, Wyoming: Geological Survey of Wyoming, Memoir 2, 151 p.

Bown, T.M., 1980, Summary of latest Cretaceous and Cenozoic sedimentary, tectonic, and erosional events, Bighorn Basin, Wyoming, *in* Gingerich, P.D., ed., Early Cenozoic Paleontology and Stratigraphy of the Bighorn Basin, Wyoming: University of Michigan, Papers on Paleontology, 24, p. 25–32.

Bown, T.M., and Kraus, M.J., 1981a, Lower Eocene alluvial paleosols (Willwood Formation, northwestern Wyoming, USA) and their significance for paleoecology, paleoclimatology, and basin analysis: Palaeogeography, Palaeoclimatology, Palaeoecology, v. 34, p. 1–30.

Bown, T.M., and Kraus, M.J., 1981b, Vertebrate fossil-bearing paleosol units (Willwood Formation, Lower Eocene, northwest Wyoming, U.S.A.): Implications for taphonomy, biostratigraphy, and assemblage analysis: Palaeogeography, Palaeoclimatology, Palaeoecology, v. 34, p. 31–56.

Bown, T.M., and Kraus, M.J., 1987, Integration of channel and floodplain suites, I. Developmental sequence and lateral relations of alluvial paleosols: Journal of Sedimentary Petrology, v. 57, p. 587–601.

Bown, T.M., and Kraus, M.J., 1993, Time-stratigraphic reconstruction and integration of paleopedologic, sedimentologic, and biotic events (Willwood Formation, lower Eocene, northwest Wyoming, U.S.A.): PALAIOS, v. 8, p. 68–80.

Bown, T.M., Rose, K.D., Simons, E.L., and Wing, S.L., 1994, Distribution and stratigraphic correlation of upper Paleocene and lower Eocene fossil mammal and plant localities of the

Fort Union, Willwood, and Tatman Formations, southern Bighorn Basin, Wyoming: U.S. Geological Survey, Professional Paper 1540, p. 1–269.

CERLING, T.E., 1992, Use of carbon isotopes in paleosols as an indicator of the $P(CO_2)$ of the paleoatmosphere: Global Biogeochemical Cycles, v. 6, p. 307–314.

CERLING, T.E., AND QUADE, J., 1993, Stable carbon and oxygen isotope in soil carbonates, *in* Swart, P.K., Lohmann, K.C, McKenzie, J., and Savin, S., eds., Climate Change in Continental Isotopic Records: American Geophysical Union, Geophysical Monograph 78, p. 217–231.

CERLING, T.E., AND WANG, Y., 1996, Stable carbon and oxygen isotopes in soil CO_2 and soil carbonate: Theory, practice, and application to some prairie soils of upper midwestern North America, *in* Boutton, T.W., and Yamasaki, S., eds., Mass Spectrometry of Soils: New York, Marcel Dekker, p. 113–131.

CLYDE, W C., STAMATAKOS, J., AND GINGERICH, P.D., 1994, Chronology of the Wasatchian Land-Mammal Age (Early Eocene): Magnetostratigraphic results from the McCullough Peaks section, northern Bighorn Basin, Wyoming: Journal of Geology, v. 102, p. 367–377.

DE CONINCK, F., 1980, Major mechanisms in the formation of spodic horizons: Geoderma, v. 24, p. 101–128.

DETTMAN, D.L., AND LOHMANN, K.C, 1993, Seasonal change in Paleogene surface water $\delta^{18}O$: Fresh-water bivalves of western North America, *in* Swart, P.K., Lohmann, K.C, McKenzie, J., and Savin, S., eds., Climate Change in Continental Isotopic Records: American Geophysical Union, Geophysical Monograph 78, p.153–163.

DEUTZ, P., MONTAÑEZ, I.P., AND MONGER, H.C., 1995, Origin of heterogeneity in carbon isotope values in pedogenic carbonate nodules from latest Pleistocene and Holocene soil; implications for paleobarometric reconstructions (Abstract): Geological Society of America, Abstracts with Programs, v. 27, no. 6, p. 205–206.

EBERL, D.D., 1993, Three zones for illite formation during burial diagenesis and metamorphism: Clay and Clay Minerals, v. 41, p. 26–37.

EBERL, D.D., VELDE, B., AND MCCORMICK, T., 1993, Synthesis of illite-smectite from smectite at earth surface temperatures and high pH: Clay Minerals, v. 28, p. 49–60.

FITZPATRICK, R.W., AND SCHWERTMANN, U., 1982, Al-substituted goethite—an indicator of pedogenic and other weathering environments in South Africa: Geoderma, v. 27, p. 335–347.

FITZPATRICK, R.W., 1988, Iron compounds as indicators of pedogenic processes: Examples from the southern hemisphere, *in* Stucki, J.W., Goodman, B.A., and Schwertmann, U., eds., Iron in Soil and Clay Minerals: Boston, D. Reidel, p. 351–396.

FREYTET, P., AND PLAZIAT, J.-C., 1982, Continental carbonate sedimentation and pedogenesis in Late Cretaceous and early Tertiary in Southern France, *in* Purser, B.H., ed., Contributions to Sedimentology: Stuttgart, E. Schweizerbart'sche Verlagsbuchhandlung, no. 12, 213 p.

FRIEDMAN, I., AND O'NEIL, J.R., 1977, Compilation of stable isotope fractionation factors of geochemical interest, *in* Fleischer, M., ed., Data of Geochemistry: U.S. Geological Survey, Professional Paper 440-KK.

GARRELS, R.M., AND CHRIST, C.L., 1965, Solutions, Minerals, and Equilibria: New York, Harper & Row, 437 p.

GHOSH, P., BHATTACHARYA, S.K., AND JANI, R.A., 1995, Palaeoclimate and palaeovegetation in central India during the Upper Cretaceous based on stable isotope composition of the palaeosol carbonates: Palaeogeography, Palaeoclimatology, Palaeoecology, v. 114, p. 285–296.

GOODFRIEND, G.A., MAGARITZ, M., AND GAT, J.R., 1989, Stable isotope composition of land snail body water and its relation to environmental waters and shell carbonate: Geochimica et Cosmochimica Acta, v. 53, p. 3215–3221.

GREENWOOD, D.R., AND WING, S.L., 1995, Eocene continental climates and latitudinal temperature gradients: Geology, v. 23, p. 1044–1048.

HEPPLE, R.P., 1995, Paleoclimatic reconstruction across the Paleocene/Eocene boundary for the Bighorn Basin of Wyoming [unpublished Bachelor's thesis]: Princeton University, Princeton, New Jersey, 78 p.

HEYES, A., AND MOORE, T.R., 1992, The influence of dissolved organic carbon and anaerobic conditions on mineral weathering: Soil Science, v. 154, p. 226–236.

HOFFMAN, J., AND HOWER, J., 1979, Clay mineral assemblages as low grade metamorphic geothermometers: Application to the thrust faulted disturbed belt of Montana, USA, *in* Scholle, P.A., and Schluger, P.R., eds., Aspects of Diagenesis: Society of Economic Paleontologists and Mineralogists,, Special Publication 26, p. 55–79.

HOWER, J., 1981, Shale diagenesis, *in* Longstaffe, F.J., ed., Clays and the Resource Geologist: Mineralogical Association of Canada, Toronto, p. 60–80.

HUMPHERY, J.D., AND FERRING, C.R., 1994, Stable isotopic evidence for latest Pleistocene and Holocene climatic change in north-central Texas: Quaternary Research, v. 41, p. 200–213.

IRWIN, H., CURTIS, C., AND COLEMAN, M., 1977, Isotopic evidence for source of diagenetic carbonates formed during burial of organic-rich sediments: Nature, v. 269, p. 209–213.

JACKSON, M.L., 1969, Soil Chemical Analysis—Advanced Course: Published by the author, University of Wisconsin, Madison, Wisconsin.

JOHNSON, D.B., AND SWETT, K., 1974, Origin and diagenesis of calcitic and hematitic nodules in the Jordan Sandstone of northeast Iowa: Journal of Sedimentary Petrology, v. 44, p. 790–794.

KLAPPA, C.F., 1978, Biolithogenesis of *Microcodium*: Elucidation: Sedimentology, v. 25, p. 489–522.

KLAPPA, C.F., 1983, A process–response model for the formation of pedogenic calcretes: Geological Society of London, Special Publication 11, p. 211–220.

KOCH, P.L., ZACHOS, J.C., AND DETTMANN, D.L., 1995, Stable isotope stratigraphy and paleoclimatology of the Paleogene Bighorn Basin (Wyoming, U.S.A.): Palaeogeography, Palaeoclimatology, Palaeoecology, v. 115, p. 61–89.

KRAUS, M.J., 1987, Integration of channel and floodplain suites, II. Vertical relations of alluvial paleosols: Journal of Sedimentary Petrology, v. 57, p. 602–612.

KRAUS, M.J., AND ASLAN, A., 1993, Eocene hydromorphic paleosols: significance for interpreting ancient floodplain processes: Journal of Sedimentary Petrology, v. 63, p. 453–463.

KRAUS, M.J., AND BOWN, T.M., 1988, Pedofacies analysis; a new approach to reconstructing ancient fluvial sequences, *in* Reinhard, J., and Sigleo, W., eds., Paleosols and Weathering through Geologic Time: Principles and Applications: Geological Society of America, Special Paper 216, p. 143–152.

KRAUS, M.J., AND BOWN, T.M., 1993, Short-term sediment accumulation rates determined from Eocene alluvial paleosols: Geology, v. 21, p. 743–746.

LANDER, R.H., 1991, White River Group diagenesis [unpublished Ph.D. thesis]: University of Illinois at Urbana–Champaign, Urbana, Illinois, 143 p.

LAWRENCE, J.R., AND RASHKES MEAUX, J., 1993, The stable isotopic composition of ancient kaolinites of North America, *in* Swart, P.K., Lohmann, K.C, McKenzie, J., and Savin, S., eds., Climate Change in Continental Isotopic Records: American Geophysical Union, Geophysical Monograph 78, p. 249–261.

LAWRENCE, J.R., AND TAYLOR, H.P., JR., 1972, Hydrogen and oxygen isotope systematics in weathering profiles: Geochimica et Cosmochimica Acta, v. 36, p. 1377–1393.

LIU, B., PHILLIPS, F.M., AND CAMPBELL, A.R., 1996, Stable carbon and oxygen isotopes of pedogenic carbonates, Ajo Mountains, southern Arizona; implications for paleoenvironmental change: Palaeogeography, Palaeoclimatology, Palaeoecology, v.124, p. 233–246.

MARKWICK, P., 1994, ''Equability'', continentality, and Tertiary ''climate'': The crocodilian perspective: Geology, v. 22, p. 613–616.

MARION, G.M., INTRONE, D.S., AND VAN CLEVE, K., 1991, The isotope geochemistry of $CaCO_3$ on the Tanana River floodplain of interior Alaska, U.S.A.: Composition and mechanisms of formation: Chemical Geology, v. 86, p. 97–110.

MCFADDEN, L.D., AND HENDRICKS, D.M., 1985, Changes in the content and composition of pedogenic iron oxyhydroxides in a chronosequence of soils in southern California: Quaternary Research, v. 23, p. 189–204.

MCKEAGUE, J.A., CHESHIRE, M.V., ANDREUX, F., AND BERTHELIN, J., 1986, Organo-mineral complexes in relation to pedogenesis, *in* Huang, P.M., and Schnitzer, M., eds., Interactions of Soil Minerals with Natural Organics and Microbes: Soil Science Society of America, Special Publication 17, p. 549–592.

MERINO, E., NAHON, D., AND WANG, Y., 1993, Kinetics and mass transfer of pseudomorphic replacement: Application to replacement of parent materials and kaolinite by Al, Fe, and Mn oxides during weathering: American Journal of Science, v. 293, p. 135–155.

MERRITTS, D.J., CHADWICK, O.A., AND HENDRICKS, D.M., 1991, Rates and processes of soil evolution on uplifted marine terraces, northern California: Geoderma, v. 51, p. 241–275.

MILLER, K.G., JANACEK, T.R., KATZ, M.E., AND KEIL, D.J., 1987, Abyssal circulation and benthic foraminiferal changes near the Paleocene/Eocene boundary: Paleoceanography, v. 2, p. 741–761.

MONGER, H.C., DAUGHERTY, L.A., AND LELAND, H.G., 1991, A microscopic examination of pedogenic calcite in an aridisol of southern New Mexico, *in* Nettleton, W.D., ed., Occurrence, Characteristics, and Genesis of Carbonate, Gypsum, and Silica Accumulations in Soils: Soil Science Society of America, Special Publication 26, p. 37–60.

MOORE, D.M., AND REYNOLDS, R.C. JR., 1989, X-ray Diffraction and the Identification and Analysis of Clay Minerals: New York, Oxford University Press, 332 p.

MORA, C.I., DRIESE, S.G., AND COLARUSSO, L.A., 1996, Middle to late Paleozoic atmospheric CO_2 levels from soil carbonate and organic matter: Science, v. 271, p. 1105–1107.

MOZLEY, P.S., AND WERSIN, P., 1992, Isotopic composition of siderite as an indicator of depositional environment: Geology, v. 20, p. 817–820.

NAHON, D.B., 1986, Evolution of iron crusts in tropical landscapes, *in* Coleman, S.H., and Dethier, D.P., eds., Rates of Chemical Weathering of Rocks and Minerals: San Diego, California, Academic Press, p. 169–191.

NAHON, D.B., HERBILLON, A.J., AND BEAUVAIS, A., 1989, The epigenetic replacement of kaolinite by lithiophorite in a manganese–lateritic profile, Brazil: Geoderma, v. 44, p. 247–259.

NARASIMHAN, T.N., GALBRAITH, R.M., WHITE, A., SMITH, A., AND SCHMIDT, H., 1982, Hydrogeochemical studies of uranium mill-tailing piles at Riverton, Wyoming and Maybell, Colorado: National Technical Information Service, Springfield VA 22161, as DE82-020572, A06 in paper copy, A01 in microfiche, LBL-14486, Annual Report for Fiscal 1981, May 1982, 93 p.

OMAR, G.I., LUTZ, T.M., AND GIEGENGACK, R., 1994, Apatite fission-track evidence for Laramide and post-Laramide uplift and anomalous thermal regime at the Beartooth overthrust, Montana–Wyoming: Geological Society of America, Bulletin, v. 106, p. 74–85.

PHILLIPS, S.E., MILNES, A.R., AND FOSTER, K.C., 1987, Calcified filaments: An example of biological influences in the formation of calcrete in south Australia: Australian Journal of Soil Research, v. 25, p. 405–428.

POLLASTRO, R.M., 1990, The illite/smectite geothermometer—concepts, methodology, and application to basin history and hydrocarbon generation, *in* Nuccio, V.F., and Barker, C.E., eds., Application of Thermal Maturation Studies to Energy Exploration: SEPM, Rocky Mountain Section, p. 1–18.

PONCET, J., 1976, Hypothèse relative à la morphogenèse du Thalle de Renalcis (algue calcaire—Paléozoïque) et affinité possible avec les Rivulariacées actuelles: Geobios, v. 9, p. 345–351.

QUADE, J., CERLING, T.E., AND BOWMAN, J.R., 1989, Systematic variation in the carbon and oxygen isotopic composition of pedogenic carbonate along elevation transects in the southern Great Basin, United States: Geological Society of America, Bulletin, v. 101, p. 464–475.

RETALLACK, G.J., 1991, Untangling the effects of burial alteration and ancient soil formation: Annual Review of Earth and Planetary Sciences, v. 19, p. 183–206.

ROBERT, M., AND BERTHELIN, J., 1986, Role of biological and biochemical factors in soil mineral weathering, *in* Huang, P.M., and Schnitzer, M., eds., Interactions of Soil Minerals with Natural Organics and Microbes: Soil Science Society of America, Special Publication 17, p. 453–495.

SAVIN, S.M., 1977, The history of the earth's surface temperature during the past 100 million years: Annual Review of Earth Planetary Sciences, v. 3, p. 319–355.

SCHLESINGER, W.H., 1985, The formation of caliche in the soils of the Mojave Desert, California: Geochimica et Cosmochimica Acta, v. 49, p. 57–66.

SCHULZE, D.G., AND DIXON, J.B., 1979, High gradient magnetic separation of iron oxides and other magnetic minerals from soil clays: Soil Science Society of America, Journal, v. 43, p. 793–799.
SCHWERTMANN, U., 1966, Inhibitory effect of soil organic matter on the crystallization of amorphous ferric hydroxide: Nature, v. 212, p. 645–646.
SCHWERTMANN, U., 1971, Transformation of hematite to goethite in soils: Nature, v. 232, p. 624–625.
SCHWERTMANN, U., 1985, The effect of pedogenic environments on iron oxide minerals: Advances in Soil Science, v. 1, p. 172–200.
SCHWERTMANN, U., AND CORNELL, R.M., 1991, Iron Oxides in the Laboratory: Preparation and Characterization: New York, VCH Publishers, 137 p.
SCHWERTMANN, U., AND FISCHER, W.R., 1973, Natural ''amorphous'' ferric hydroxide: Geoderma, v. 10, p. 237–247.
SCHWERTMANN, U., AND MURAD, E., 1983, Effect of pH on the formation of goethite and hematite from ferrihydrite: Clays and Clay Minerals, v. 31, p. 277–284.
SCHWERTMANN, U., AND TAYLOR, R.M., 1989: Iron oxides, *in* Dixon, J.B., and Weed, S.B., eds., Minerals in Soil Environments: Soil Science Society of America, Book Series, v. 1, p. 379–438.
SCHWERTMANN, U., FITZPATRICK, R., TAYLOR, R.M., AND LEWIS, D.G., 1979, The influence of aluminum on iron oxides. Part II: Preparation and properties of Al-substituted hematites: Clays and Clay Minerals, v. 27, p. 105–112.
SCHWERTMANN, U., KODAMA, H., AND FISCHER, W.R., 1986, Mutual interactions between organics and iron oxides, *in* Huang, P.M., and Schnitzer, M., eds., Interactions of Soil Minerals with Natural Organics and Microbes: Soil Science Society of America, Special Publication 17, p. 223–250.
SCHWERTMANN, U., MURAD, E., AND SCHULZE, D.G., 1982, Is there Holocene reddening (hematite formation) in soils of axeric temperate areas?: Geoderma, v. 27, p. 209–223.
SHACKLETON, N.J., AND KENNETT, J.P., 1975, Paleotemperature history of the Cenozoic and the initiation of Antarctic glaciation; oxygen and carbon isotope analyses in DSDP sites 277, 279, and 281, *in* Deep Sea Drilling Project, Initial Reports, v. 29, p. 743–755.
SINGH, B., AND GILKES, R.J., 1992, Properties and distribution of iron oxides and their association with minor elements in the soils of south-western Australia: Journal of Soil Science, v. 43, p. 77–98.
SINHA, A. AND STOTT, L.D., 1994, New atmospheric pCO_2 estimates from Paleosols during the late Paleocene/early Eocene global warming interval: Global and Planetary Change, v. 9, p. 297–307.
STERN, L.A., CHAMBERLAIN, C.P., AND JOHNSON, G.D., 1995, Record of climate change preserved in oxygen isotope systematics of pedogenic clay minerals in Himalayan molasse (abstract): Geological Society of America, Abstracts with Programs, v. 27, no. 6, p. 206.
STOTT, L.D., KENNETT, J.P., SHACKLETON, N.J., AND CORFIELD, R.M., 1990, The evolution of Antarctic surface waters during the Paleogene: Inferences from the stable isotopic composition of planktonic foraminifera, *in* Barker, P.F., and Kennett, J.P. et al., eds., Proceedings of Ocean Drilling Program, Science Results, v. 113, p. 849–864.
TAN, K.H., 1986, Degradation of soil minerals by organic acids, *in* Huang, P.M., and Schnitzer, M., eds., Interactions of Soil Minerals with Natural Organics and Microbes: Soil Science Society of America, Special Publication 17, p. 1–27.
TAN, K.H., 1989, Role of humic and fulvic acids in mineral weathering: Clay Research, v. 8, p. 11–20.
TAUXE, L., GEE, J., GALLET, Y., PICK, T., AND BOWN, T., 1994, Magnetostratigraphy of the Willwood Formation, Bighorn Basin, Wyoming: New constraints on the location of Paleocene/Eocene boundary: Earth and Planetary Science Letters, v. 125, p. 159–172.
VAN HOUTEN, F.B., 1944, Stratigraphy of the Willwood and Tatman formations in northwestern Wyoming: Geological Society of America, Bulletin, v. 55, p. 165–210.
VEPRASKAS, M.J., AND GUERTAL, W.R., 1992, Morphological features of soil wetness, *in* Kimble, J.M., ed., Proceedings of the Eighth International Soil Correlation Meeting (VIII ISCOM): Characterization, Classification, and Utilization of Wet Soils: Lincoln, Nebraska, U.S. Department of Agriculture, Soil Conservation Service, National Soil Survey Center, p. 307–312.
WANG, M.K., AND HSU, P.H., 1980, Effects of temperature and iron(III) concentration on the hydrolytic formation of iron(III) oxyhydroxides and oxides: Soil Science Society of America, Journal, v. 44, p. 1089–1095.
WEEKS, L.G., 1953, Environment and mode of origin and facies relationships of carbonate concretions in shales: Journal of Sedimentary Petrology, v. 23, p. 162–173.
WING, S.L., 1991, Comments and reply on '''Equable' climates during Earth history?'': Geology, v. 19, p. 539–542.
WING, S.L., AND GREENWOOD, D.R., 1993, Fossils and fossil climate: the case for equable continental interiors in the Eocene: Royal Society [London], Philosophical Transactions, ser. B, v. 341, p. 243–252.
WING, S.L., BOWN, T.M., AND OBRADOVICH, J.D., 1991, Early Eocene biotic and climatic change in interior western North America: Geology, v. 19, p. 1189–1192.
WINOGARD, I.J. AND ROBERTSON, F.N., 1982, Deeply oxygenated ground water: anomaly or common occurrence?: Science, v. 216, p. 1227–1230.
WOLFE, J.A., 1978, A paleobotanical interpretation of Tertiary climates in the northern hemisphere: American Scientist, v. 66, p. 694–703.
WOLFE, J.A., 1994, Tertiary climatic changes at middle latitudes of western North America: Palaeogeography, Palaeoclimatology, Palaeoecology, v. 108, p. 195–205.
YAPP, C.J., 1979, Oxygen and carbon isotope measurements of land snail shell carbonate: Geochimica et Cosmochimica Acta, v. 43, p. 629–636.
YAPP, C.J., 1987, Oxygen and hydrogen isotope variations among goethites (α-FeOOH) and the determination of paleotemperatures: Geochimica et Cosmochimica Acta, v. 51, p. 355–364.
YAPP, C.J., 1991, Oxygen isotopes in an oolitic ironstone and the determination of goethite $\delta^{18}O$ values by selective dissolution of impurities: The 5 *M* NaOH method: Geochimica et Cosmochimica Acta, v. 55, p. 2627–2634.
YAPP, C.J., 1993a, The stable isotope geochemistry of low temperature Fe(III) and Al ''oxides'' with implications for continental paleoclimates, *in* Swart, P.K., Lohmann, K.C, McKenzie, J., and Savin, S., eds., Climate Change in Continental Isotopic Records: American Geophysical Union, Geophysical Monograph 78, p. 285–294.
YAPP, C.J., 1993b, Paleoenvironmental and the oxygen isotope geochemistry of ironstone of the Upper Ordovician Neda Formation, Wisconsin, USA: Geochimica et Cosmochimica Acta, v. 57, p. 2319–2327.
YAPP, C.J., 1997, An assessment of isotopic equilibrium of goethites from a bog iron deposits and a lateritic regolith: Chemical Geology, v. 135, p. 159–171.
YONGE, C.J., FORD, D.C., GRAY, J., AND SCHWARCZ, H.P., 1985, Stable isotope studies of cave seepage water: Chemical Geology, v. 58, p. 97–105.
ZACHOS, J.C., LOHMANN, K.C, WALKER, J.C.G., AND WISE, S.W., 1993, Abrupt climate change and transient climates in the Paleogene: A marine perspective: Journal of Geology, v. 100, p. 191–213.

Received 25 September 1997; accepted 4 March 1998.